Shear Stress-Driven Refreshing Capability of Plastic Deformation in Nanolayered Metals

J. W. Yan, X. F. Zhu, B. Yang, and G. P. Zhang*

Shenyang National Laboratory for Materials Science, Institute of Metal Research, Chinese Academy of Sciences, 72 Wenhua Road, Shenyang 110016, People's Republic of China

(Received 15 December 2012; published 9 April 2013)

Severely localized deformation within shear bands can occur much more easily in a metal with nanoscale microstructures, such as nanograined and nanolayered materials. Based on atomic-scale observations, here we show that such locally large deformation (the continuous thinning of the layers) within the indentation-induced shear bands of the Cu/Au nanolayers is essentially attributed to the large shear stress component along the interface, which can refresh the capability of the interface to absorb incoming dislocations through unlocking the product of the dislocation-interface reaction. The results have implications for understanding the interface-mediated mechanisms of plastic deformation and for the engineering application of severe plastic deformation processing of metals at nanoscales.

DOI: 10.1103/PhysRevLett.110.155502 PACS numbers: 62.25.−g, 68.60.Bs, 68.65.Ac

The interface, as a boundary between two phases, grains and heterogeneous materials, plays a key role in the mechanical performance of materials. Nanostructured metals (such as nano- or ultrafine-grained and nanolayered metals) characterized structurally by a large volume fraction of grain boundaries and/or interfaces usually exhibit an ultrahigh strength [1–3]. However, these materials often have a limited ductility due to the occurrence of unstable plastic deformation corresponding to the onset of shear bands (SBs) [4]. Shear banding is usually a dangerous deformation behavior characterized by the development of a locally large strain with a small volume. In nanocrystalline Fe, it was reported that the number of SBs increased with applied strain [5], and the grains inside the SB were elongated and contained high dislocation densities compared to equiaxed grains outside the SBs [6]. In some metallic nanolayers, the shear banding behavior was also observed frequently [7–11]. The number of SBs could increase with decreasing individual layer thickness, and it is easier for the SBs to form in nanolayers with face centered cubic (fcc)-fcc interfaces than that in nanolayers with fcc-body centered cubic interfaces [12]. However, one would question why there is a large capability of plastic deformation inside the SBs. Some evidence suggested that grain boundary-mediated deformation, such as grain boundary sliding, grain rotation [7,10], and unbalanced slip of intralayer slip systems [9], could occur in the SBs. This Letter presents a finding on the origin of the large plastic deformation within such SBs in the Cu/Au nanolayers by means of atomic-scale observations of the interaction between the dislocation and the interface. We demonstrate that the shear stress along the interface could unlock the production of the dislocation-interface reaction, and that enhances the ability of the metallic nanolayers to plastically flow inside SBs.

1 μm-thick Cu/Au multilayers with a nominal individual layer thickness of 25 nm were deposited on 525 μm-thick single-crystal Si substrates under ultrahigh vacuum (base pressure $< 10^{-7}$ Torr) using dc magnetron sputtering. Both Au and Cu layers consist of regular columnar grains with an in-plane size of about 80 nm [13]. After a locally large plastic deformation was introduced into the nanolayers by microindentation (1 N load for 13 s holding time), multiple SBs corresponding to circular pileups around the indent appeared [Fig. 1(a)]. Owing to the confinement of the substrate and the surrounding layers, the nanolayers in the confined zone (CZ) (region A) and pileup zone (region B) shown in Fig. 1(a) were simultaneously subjected to both of compressive stress (σ_c) and shear stress (τ) components along the interface. Transmission electron microscopy observations show that the layers in region A were thinned uniformly [Fig. 1(b)], while those in region B have been kinked and elongated severely toward the SB direction [Fig. 1(c)]. In such a small confined volume, the Cu layers marked by 1, 2, and 3 were actually subjected to shear strain of about 2.35, 2.61, and 2.87, respectively, along the SB direction and the elongation of the kinked layers is about 1.38, 1.45, and 1.68, respectively, showing an extremely large ability for local plastic deformation.

To quantify the thinning behavior of the nanolayers, the distribution of Au and Cu elements in the CZ was first visualized by a high angle annular dark field image and energy dispersive x-ray spectroscopy (EDS) mapping analysis in the scanning transmission electron microscope (STEM) mode, as shown in Figs. 2(a) and 2(b) for the layers before and after deformation, respectively. Furthermore, the average individual layer thicknesses before (λ) and after (λ^*) indentation were determined based on the full width at half maximum on the line scanning profile of the layers taken by EDS line-scan measurements in the STEM mode, and plotted in Fig. 2(c). It is clear that both of the Au and Cu layers in the CZ and the SB became thinned after indentation, but the Au layer was thinned more than the Cu layer in the CZ,

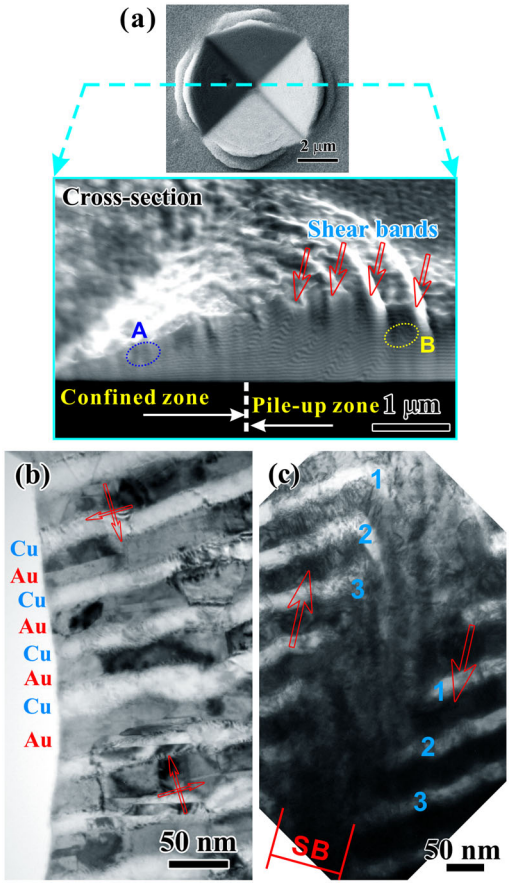

FIG. 1 (color online). (a) Scanning electron microscope plan view and focused ion beam cross-sectional view of shear banding behavior beneath an indent, transmission electron microscopy images of the deformed Cu/Au nanolayers (b) in confined zone and (c) within shear bands.

while the Cu layer was thinned more severely than the Au layer in the SB, indicating the different extent of layer thinning in both zones.

We first consider variations in layer thickness in a Cu/Au bilayer unit subjected to σ_c only [Fig. 2(d)]. The indentation-induced global compressive strain (ε_c) of the bilayer unit is estimated by the variation in the bilayer thickness before (Λ) and after (Λ^*) indentation as, $\varepsilon_c = \frac{\Lambda^* - \Lambda}{\Lambda}$. Then, a relation between ε_c and the compressive strains of the Au layer ($\varepsilon_{\mathrm{Au}}$) and the Cu layer ($\varepsilon_{\mathrm{Cu}}$) can be written as,

$$\varepsilon_c = \frac{\lambda_{\mathrm{Au}}(1+\varepsilon_{\mathrm{Au}}) + \lambda_{\mathrm{Cu}}(1+\varepsilon_{\mathrm{Cu}}) - \Lambda}{\Lambda}. \quad (1)$$

The strain in the CZ was accommodated by the cooperative deformation of the Cu and Au layers in the equal-stress condition of a composite [14], and thus can be estimated by their elastic moduli as

$$\frac{\varepsilon_{\mathrm{Au}}}{\varepsilon_{\mathrm{Cu}}} = \frac{E_{\mathrm{Au}}}{E_{\mathrm{Cu}}}. \quad (2)$$

Based on Eqs. (1) and (2), we got $\varepsilon_c = -0.256$, $\varepsilon_{\mathrm{Au}} = -0.263$, and $\varepsilon_{\mathrm{Cu}} = -0.106$ in the CZ. Using $\varepsilon_{\mathrm{Au}}$ and $\varepsilon_{\mathrm{Cu}}$, the thicknesses of the Au and Cu layers in the CZ were calculated as $\lambda'_{\mathrm{CZ,Au}} = 28.70$ and $\lambda'_{\mathrm{CZ,Cu}} = 21.26$ nm, respectively. However, we found that a difference $(\lambda^*_{\mathrm{CZ,Au}} - \lambda'_{\mathrm{CZ,Au}})$ between the calculated value $\lambda'_{\mathrm{CZ,Au}}$ (only σ_c without τ) and the measured value $\lambda^*_{\mathrm{CZ,Au}}(\sigma_c$ and $\tau)$ for the Au layer is 0.757 nm, while that $(\lambda^*_{\mathrm{CZ,Cu}} - \lambda'_{\mathrm{CZ,Cu}})$ for the Cu layer is -0.757 nm. This means that when both the Au and the Cu layers in the CZ were thinned simultaneously, the Cu layer was additionally thinned about 0.757 nm due to the involvement of τ besides the thinning from $\lambda_{\mathrm{Cu}} = 23.8$ nm to $\lambda'_{\mathrm{CZ,Cu}} = 21.26$ nm due to σ_c, the Au layer actually became thickened additionally 0.757 nm due to τ. Such an analysis reveals that it is the *shear stress* along the Cu/Au interface, namely interface shear stress (ISS), that leads to the additional thinning of the nanolayers.

A question is why the ISS can enhance plastic flow of the nanoscale layers through continuous thinning of the layers in addition to σ_c-induced thinning. A high resolution electron microscope image [Fig. 3(a)] shows that before deformation the nanolayers has a perfectly transparent interface with an orientation relationship, $\{111\}_{\mathrm{Cu}}//\{111\}_{\mathrm{Au}}$ and $\langle 110\rangle_{\mathrm{Cu}}//\langle 110\rangle_{\mathrm{Au}}$. No disconnections were observed at the interface [Fig. 3(b)] when we took a close examination on the dotted-square region in Fig. 3(a). In comparison, after indentation deformation two ledges (disconnections) have formed at the interface in the CZ [Fig. 3(c)]. The height of the ledge measured from the high resolution electron microscope image is of the scale of two atomic layers. Two stacking-fault layers starting right from the interface ledge were also found in the Cu layers. A Frank circuit around the interface step along the (111) and $(11\bar{1})$ lattice fringes in both Au and Cu layers was not closed [Fig. 3(d)], and the closure failure was measured as about $\frac{1}{12}[\bar{1}\,\bar{1}\,2]$, indicating the existence of a partial dislocation with a Burgers vector of $b = \frac{1}{6}[\bar{1}\,\bar{1}\,2]$. We expect that the partial dislocation is the product of the dislocation-interface interaction.

Figure 4 schematically illustrates all perfect and partial dislocations on slip planes in the Cu and Au layers with the (111) interface plane ABC using the double Thompson tetrahedrons [15]. We suggest that the observed interface ledges were induced through the following processes of the dislocation-interface interaction described in Fig. 5. At the onset of plastic deformation, a full dislocation DC with a Burgers vector of $b = \frac{1}{2}[110]a_{Cu}$ in the Cu layer was driven to the interface by the applied stress [Fig. 5(a)], and dissociated into a leading 30° (αC) and a trailing 90° ($D\alpha$) partial dislocations [Fig. 5(b)]. The 30° leading partial αC on the slip plane BCD met the interface plane ABC first, and then released a partial dislocation δC on the interface through the dislocation-interface reaction [Fig. 5(c)]. $\alpha\delta$ is a stair-rod dislocation left at the interface

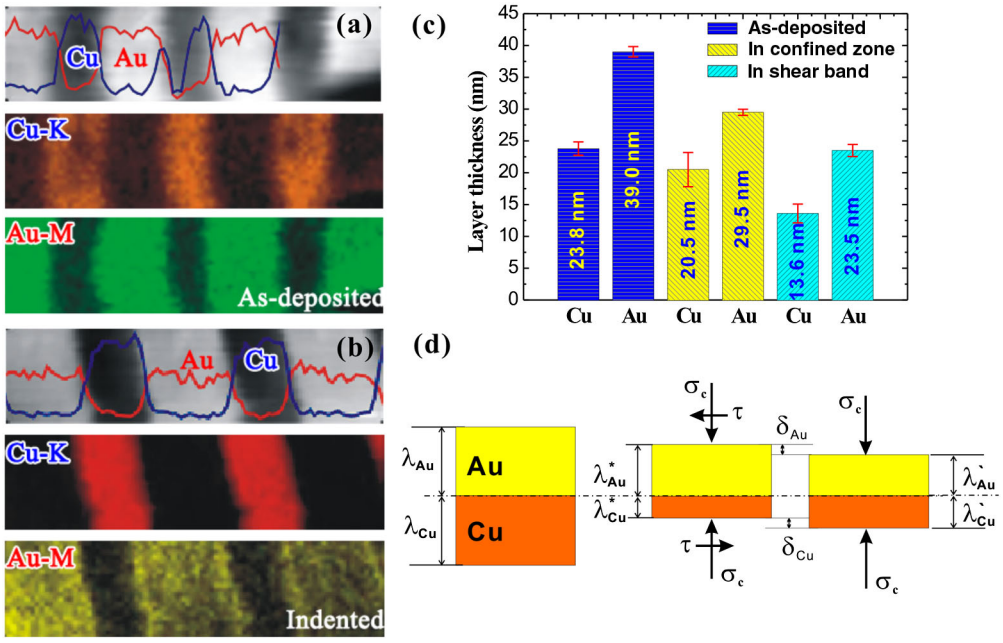

FIG. 2 (color online). High angle annular dark field images [the first image in (a) and (b)] and Cu-K and Au-M elemental maps [the second and the third images in (a) and (b)] in the STEM mode demonstrating the distribution of Au and Cu elements (a) before deformation and (b) after deformation. Line profiles of the local Cu and Au layers were taken by EDS line-scan measurements. (c) Variation of thickness of Au and Cu layers in confined zone and shear band before and after indentation deformation. The standard errors are also shown by red bars. (d) Schematic illustration of comparison of the layer thickness of a Cu/Au bilayer unit subjected to only a normal compressive stress (σ_c) and normal compressive stress + shear stress (τ), respectively.

[Fig. 5(c)]. Under the ISS, the partial δC would glide along the interface starting from the interface step, leaving a stacking fault behind [the shadow area in Fig. 5(c)], while the trailing 90° partial $D\alpha$ would be dissociated following the reaction (3) in Fig. 5(d). Here, $\delta\alpha$ is another stair-rod dislocation and can annihilate as meeting $\alpha\delta$ formed previously in the reaction (2). $D\delta$ [Fig. 5(d)] in the Cu layer is an edge dislocation with $b = \frac{1}{3}[111]a_{\mathrm{Cu}}$, and has the same direction as $\delta' D'$ in the Au layer except that the magnitudes of the Burgers vectors are different. Thus, $D\delta$ may cross the interface through the reaction (4) in Fig. 5(e), where $\delta\delta'$ is the residual dislocation at the interface. The transmission of $D\delta$ would leave an offset at the interface depicted in Fig. 5(e), and the height of such the step is of the magnitude of $b = \frac{1}{3}\langle 111\rangle$ of $D\delta$, which is the thickness of two atomic layers along the [111] direction. It is expected that $D\delta$ crossing the interface was promoted once the partial δC was pushed away from $D\delta$ under the certain ISS. This can be understood by evaluating the interaction energy per unit length (W/L) between two general parallel dislocations b_1 and b_2 as a function of their separation, R [16]:

$$\frac{W}{L} = \frac{\mu(b_1\xi)(b_2\xi)}{2\pi}\ln\frac{R}{R_a} - \frac{\mu}{2\pi(1-\nu)}[(b_1\times\xi)(b_2\times\xi)] \times \ln\frac{R}{R_a} - \frac{\mu}{2\pi(1-\nu)R^2}[(b_1\times\xi)R][(b_2\times\xi)R], \quad (3)$$

where μ is shear modulus, ν is Poisson ratio, R_a is the initial spacing between the two interacting dislocations and ξ is the dislocation line direction. Substituting the parameters for $D\delta$ with $b_1 = \frac{1}{3}[111]$ and δC with $b_2 = \frac{1}{6}[\bar{1}\,\bar{1}\,2]$, and the dislocation line direction ξ being parallel to the electron beam direction ($[1\bar{1}0]$), the interaction energy becomes

$$\frac{\mathbf{W}}{L} = -\frac{\boldsymbol{\mu}}{2\boldsymbol{\pi}(\mathbf{1}-\boldsymbol{\nu})}[(\mathbf{b}_1\times\boldsymbol{\xi})\cdot(\mathbf{b}_2\times\boldsymbol{\xi})]\ln\frac{\mathbf{R}}{\mathbf{R}_a}. \quad (4)$$

Evidently, the total interaction energy will decrease as R increases; i.e., the partial δC was pushed away by the ISS. This indicates that the ISS is indeed beneficial to $D\delta$ crossing the interface. Of course, the stacking fault would expand as the partial δC glides over a distance R on the interface plane, resulting in the increase of the system energy. Thus, the partial δC may not glide unlimitedly.

It should be mentioned that the Burgers vector of $D\delta$ is perpendicular to its slip plane, meaning $D\delta$ can only climb instead of gliding. The transmission of $D\delta$ from the Cu layer to the Au layer would lead to a decrease in the dislocation line energy, which makes the transmission energy more favorable. The residual dislocation $\delta\delta'$ has $b = \frac{1}{3}[111](a_{\mathrm{Cu}} - a_{\mathrm{Au}})$, and may be dissolved into the coherent strain at the Cu/Au interface. Furthermore, the dislocation $\delta' D'$ in the Au layer could then release another partial dislocation through the reaction (5), and generate a stair-rod dislocation $\delta' C'$ at the interface step and a perfect

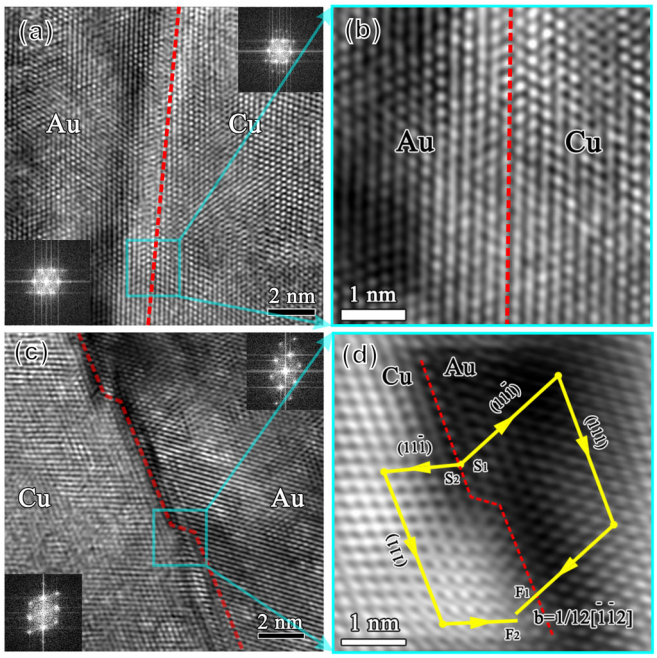

FIG. 3 (color online). High resolution electron microscope observations on Cu/Au interface structures of (a) and (b) before, and (c) and (d) after indentation deformation. The images were taken along the [110] zone axis for both layers.

dislocation $C'D'$ in the Au layer at the same time [Fig. 5(f)]. Obviously, in the above process it was the ISS that enhanced the capability of the heterogeneous interface to absorb lattice dislocations through the fact that the ISS pushed the partial dislocations at the interface away from the sink, and thus assisted $D\delta$ crossing.

In the SB, the fact that the Cu layer could become much thinner than the Au layer [Fig. 2(c)] indicates that the ISS-driven mechanism becomes more active than that in the CZ. Under the indentation load, the σ_c-induced layer thinning led to strain hardening, making the deformation of the nanolayers difficult gradually, while the rotation of the layers within SBs toward the shear direction [about 54° relative to the interface plane in Fig. 1(c)] gradually increases the ISS, which promoted $D\delta$ crossing the interface and the ability for the interface to absorb incoming

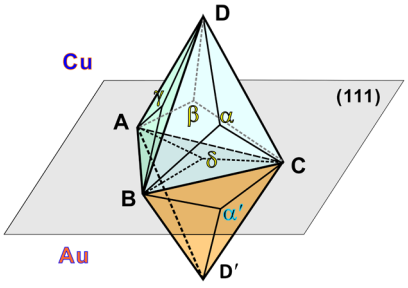

FIG. 4 (color online). Double Thompson tetrahedrons depicting all perfect and partial dislocations on slip planes in the Cu and Au layers, which have the (111) interface plane ABC.

dislocations, making interface-mediated plasticity more active. An elasticity-based model predicted that the attractive interaction for a dislocation toward a shearable interface (Cu/Nb nanolayers) could be effective in depleting glide dislocations within the nanolayers when the layers become sufficiently thin [17]. Similarly, the present interface could also deplete glide dislocations within the layers assisted by the external ISS, leading to the evident elongation of the nanolayers in the SBs.

The fact that the larger local strain can develop inside SBs may provide a new clue that the nanolayers are not intrinsically brittle but *deformable* actually under high compressive constraint. The nanoscale coherent twin boundary can serve as both an obstacle to the dislocation transmission and sources and/or sinks of dislocations [18], while our finding reveals that the heterogeneous Cu/Au interface may also act as the fresh sink to continuously absorb the lattice dislocations into the interface as long as the ISS could unlock the dislocation-interface reaction-produced dislocation ($D\delta + \delta C$) configuration residing at the interface. This permits more lattice dislocations inside the nanoscale layers to sink in the interface. Consequently, the continuous thinning of the layers in SBs can go on further at the nanoscale level. Following such a deformation criterion, we expect that some resolved shear stresses would inevitably be imposed on some GBs in bulk nanograined materials (especially within SBs) due to the random distribution of the GB orientations, and that promotes the preferential deformation of some grains along the shear direction once the ISS could facilitate the dislocation-interface interaction. This may provide an explanation to why the nanograins are deformed and

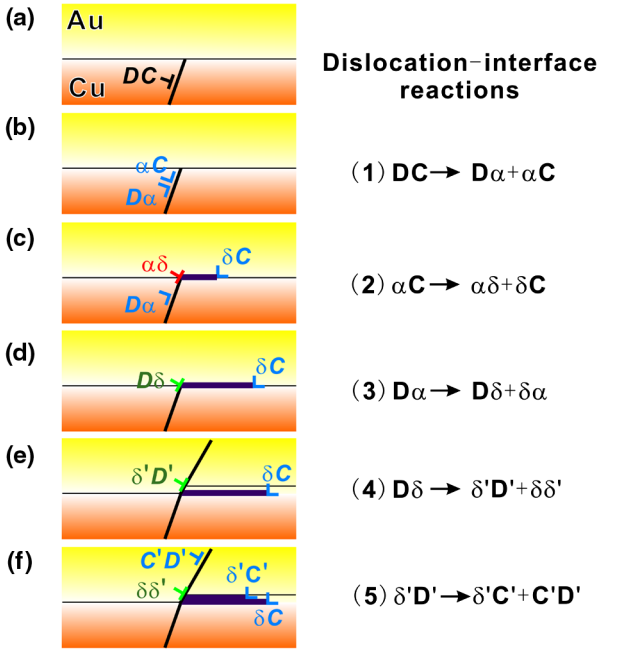

FIG. 5 (color online). Schematic illustration of the process of dislocation-interface reactions in the Cu/Au nanolayers.

elongated preferentially within SBs oriented along the shear direction [6].

Furthermore, the new mechanism on shear stress-driven interface-mediated plasticity in the confined nanolayers may also have implications for the applications in severe plastic deformation processing of engineering materials with layered structures, such as pearlitic steels, α/β lamellar Ti alloys, and eutectic alloys, etc. We expect that mechanical processing with a magnitude of the ISS may promote the plastic flow of the layer-structured materials at nanoscales. In fact, a surprising ability to produce the nanoscale microstructures in some metals and alloys using severe plastic deformation [19] and heavily cold-drawing techniques [20] might be related to the shear stress-driven interface plasticity.

In summary, our results reveal that the locally large strain within the indentation-induced SBs of the Cu/Au nanolayers is essentially attributed to the large ISS, which can refresh the capability for incoming dislocations to be absorbed into the interface through unlocking the product of the dislocation-interface reaction. The findings in this Letter shed new insight into the fundamentals of plastic deformation of nanolayered materials, which may help to guide designing and processing nanostructured materials.

This work was supported by the National Natural Science Foundation of China (NSFC, Grants No. 50971125, No. 50890173, and No. 51001105), the National Basic Research Program of China (Grant No. 2010CB631003) and partially supported by the NSFC (Grant No. 51071158).

*Corresponding author.
gpzhang@imr.ac.cn

[1] M. A. Meyers, A. Mishra, and D. J. Benson, Prog. Mater. Sci. **51**, 427 (2006).
[2] B. M. Clemens, H. Kung, and S. A. Barnett, MRS Bull. **24**, 20 (1999).
[3] R. G. Hoagland, R. J. Kurtz, and C. H. Henager, Scr. Mater. **50**, 775 (2004).
[4] E. Ma, J. Minerals, Metals and Materials Soc. **58**, 49 (2006).
[5] Q Wei, L. Kecskes, T. Jiao, K. T. Hartwig, K. T. Ramesh, and E. Ma, Acta Mater. **52**, 1859 (2004).
[6] D. Jia, K. T. Ramesh, and E. Ma, Acta Mater. **51**, 3495 (2003).
[7] G. P. Zhang, Y. Liu, W. Wang, and J. Tan, Appl. Phys. Lett. **88**, 013105 (2006).
[8] D. Bhattacharyya, N. A. Mara, P. Dickerson, R. G. Hoagland, and A. Misra, J. Mater. Res. **24**, 1291 (2009).
[9] N. A. Mara, D. Bhattacharyya, J. P. Hirth, P. Dickerson, and A. Misra, Appl. Phys. Lett. **97**, 021909 (2010).
[10] Y. P. Li, X. F. Zhu, G. P. Zhang, J. Tan, W. Wang, and B. Wu, Philos. Mag. **90**, 3049 (2010).
[11] D. Wang, T. Kups, J. Schawohl, and P. Schaaf, J. Mater. Sci.: Mater. El **23**, 1077 (2012).
[12] Y. P. Li, X. F. Zhu, J. Tan, B. Wu, W. Wang, and G. P. Zhang, J. Mater. Res. **24**, 728 (2009).
[13] Y. P. Li and G. P. Zhang, Acta Mater. **58**, 3877 (2010).
[14] M. A. Meyers and K. K. Chawla, *Mechanical Behavior of Materials* (Cambridge University Press, Cambridge, England, 2009).
[15] C. S. Hartley and D. L. A. Blachon, J. Appl. Phys. **49**, 4788 (1978).
[16] F. Nabarro, Adv. Phys. **1**, 269 (1952).
[17] R. G. Hoagland, R. J. Kurtz, and C. H. Henager, Scr. Mater. **50**, 775 (2004).
[18] L. Lu, X. Chen, X. Huang, and K. Lu, Science **323**, 607 (2009).
[19] R. Z. Valiev, R. K. Islamgaliev, and I. V. Alexandrov, Prog. Mater Sci. **45**, 103 (2000).
[20] X. D. Zhang, A. Godfrey, X. Huang, N. Hansen, and Q. Liu, Acta Mater. **59**, 3422 (2011).